PHYSICAL REVIEW B VOLUME 38, NUMBER 17 15 DECEMBER 1988-I

Capacitance measurements of magnetic localization and magnetic freezeout in n^--type GaAs

T. W. Hickmott
IBM Research Division, Thomas J. Watson Research Center, P.O. Box 218, Yorktown Heights, New York 10598

(Received 10 November 1987; revised manuscript received 4 March 1988)

dc resistance and Hall-effect measurements are conventionally used to study magnetoresistance in lightly doped semiconductors. In the present paper, ac capacitance-voltage (C-V) and conductance-voltage (G-V) measurements on n^--type GaAs–$Al_xGa_{1-x}As$–n^+-type-GaAs (hereafter abbreviated as AlGaAs) capacitors are used to study magnetic localization and magnetic freezeout in bulk n^--type GaAs at temperatures between 1.4 and 4.2 K and in magnetic fields B up to 14 T. Detailed results are given on two samples whose dopings are 1.7×10^{15} and 7×10^{15} cm^{-3}. For the more lightly-doped sample, an exponential magnetoresistance of n^--type GaAs is due to magnetic localization. There is good agreement between experimental results and the percolation theory of hopping conduction in lightly doped semiconductors of Shklovskii and Efros, and of Ioselevich. For the more heavily-doped sample, a dip is observed at flat-band voltage in C-V curves for $B \gtrsim 6$ T. The dip is due to magnetic freezeout in n^--type GaAs which lowers the carrier concentration and moves the Fermi level into the lower impurity band. Although the mechanisms responsible for magnetoresistance differ for the two samples, the activation energy for magnetoresistance, $\varepsilon_3=0.4$–0.6 meV, is the same in the magnetic field region where the data overlap. The results validate the use of C-V and G-V measurements on AlGaAs capacitors for quantitative measurements of magnetoresistance in bulk GaAs.

INTRODUCTION

The effect of magnetic fields on conduction in lightly doped semiconductors (such as InSb, InP, or GaAs) has been extensively studied because of its relation to the problems of localization, the metal-insulator transition, and magnetic freezeout.[1-4] Most experimental studies of magnetoconduction in lightly doped GaAs have used Hall-effect and dc resistance measurements to study conduction at low temperatures and high magnetic fields.[5-15] Capacitance measurements on bulk samples have been used to study the metal-insulator transition in several systems; for example, in heavily doped GaAs (Ref. 16) and in Si:P.[17,18] Hopping conductivity has been studied in n^+-type-GaAs–n^--type-GaAs–n^+-type-GaAs capacitors.[19-21] In the present work we have used capacitance-voltage (C-V) and conductance-voltage (G-V) measurements on n^--type-GaAs-undoped-$Al_xGa_{1-x}As$–n^+-type-GaAs (hereafter abbreviated as AlGaAs) capacitors to study magnetoresistance of n^--type GaAs. The results have implications for understanding both the behavior of GaAs/$Al_xGa_{1-x}As$ heterostructures in high magnetic fields and for the nature of conduction processes in lightly doped GaAs.

A lightly doped semiconductor such as n^--type GaAs is characterized by its donor concentration N_D, by the donor-energy separation from the conduction band E_D, by the compensation $K=N_A/N_D$, where N_A is the acceptor concentration, and by the effective Bohr radius $a_H^*=\hbar^2\kappa/m^*e^2$. κ is the dielectric constant of the semiconductor, e is the electric charge, and m^* is the effective mass of electrons. At low temperatures, hopping conduction occurs for low impurity doping, $N_D^{1/3}a_H^*\sim0.1$, and $0.1\lesssim K\lesssim0.9$.[4] In this concentration regime the overlap of electron wave functions on neighboring donors is small; electrons are localized. They move from an occupied donor to an empty donor by tunneling and conduction is thermally activated. For large donor concentrations metallic conduction is observed; conduction is not thermally activated. The Mott criterion for the metal-insulator transition in n^--type GaAs, $N_D^{1/3}a_H^*\sim0.25$,[22] is satisfied for $N_D\sim1.6\times10^{16}$ cm^{-3}, assuming that $\kappa=12.5$ and $m^*=0.067m_0$, where m_0 is the mass of a free electron in vacuum. Conduction for lower values of N_D is through impurity bands.

A characteristic feature of hopping conduction in doped semiconductors is a giant positive magnetoresistance which depends exponentially on magnetic field.[23] The effect of the magnetic field B on hopping conduction is due to *magnetic localization;* the magnetic field shrinks the electron radius, reduces overlap of the electron wave function with empty donors, and thus makes it harder for carriers to tunnel from a full donor to an empty donor. Shlovskii and Efros,[4] Shklovskii,[24-26] and Pollak[27] have treated the effect of magnetic field on hopping conduction in lightly doped semiconductors as a percolation problem. They derived expressions for magnetoresistence in weak field and in strong field. Ioselevich[28] has extended their analysis to the case of an arbitrary magnetic field. Chroboczek[29] has compared the results of Kahlert *et al.*[10] on magnetoresistance of epitaxial GaAs layers with the theory of Refs. 23 and 28. Chroboczek *et al.*[20] have analyzed the effect of magnetic field on ac-conductance measurements on n^+-n^--n^+ GaAs mesa structures. In both

 ©1988 The American Physical Society

cases agreement between theory and experiment is only fair.

Magnetoresistance due to *magnetic localization* in lightly doped semiconductors can be contrasted to *magnetic freezeout* of electrons which occurs at higher magnetic fields than are required to observe magnetic localization. Yafet, Keyes, and Adams (YKA) (Ref. 30) first discussed magnetic freezeout in semiconductors in connection with the behavior of a hydrogen atom in a magnetic field. The cyclotron radius of an electron in a doped semiconductor in a magnetic field B is given by $L=(\hbar/eB)^{1/2}$ and the cyclotron energy is given by $\hbar\omega_c=eB\hbar/m^*$. YKA showed that if $\gamma=\hbar\omega_c/2\mathcal{R}\gtrsim 1$, where $\mathcal{R}$ is the Rydberg energy of a donor, then magnetic freezeout of electrons onto donors can occur. Magnetic freezeout occurs when L becomes comparable to a_H^*; for n^--type GaAs with $E_D\sim 5.75$ meV $a_H^*=9.8$ nm, and freezeout occurs for $B\gtrsim 6.4$ T. The effect of magnetic freezeout is to reduce the concentration of carriers in a conduction band by neutralizing positive ionized donors. Magnetic freezeout also increases the donor binding energy.

The AlGaAs capacitor, shown schematically in Fig. 1(a), is one of the simplest single-barrier heterostructures. For B perpendicular to an AlGaAs capacitor and positive voltage biases on the n^+-type GaAs gate that produce an accumulation layer on n^--type GaAs, C-V, G-V, and current-voltage (I-V) curves show structure due to Landau levels of the two-dimensional electron gas of the accumulation layer.[31] For negative voltage biases that produce a depletion layer in n^--type GaAs, structure is observed in C-V, G-V, and I-V curves of some samples due to LO phonons.[32] There is also a marked decrease in capacitance at high magnetic fields which has been attributed to magnetic freezeout in n^--type GaAs.[31] Eaves *et al.*[33] pointed out that magnetoresistance due to magnetic localization in n^--GaAs was not considered and that the equivalent circuit of the AlGaAs capacitor is more complicated than the one used in Refs. 31 and 32.

In the present work C-V and G-V measurements of AlGaAs capacitors are used for quantitative studies of magnetic localization and magnetic freezeout in n^--type GaAs. Detailed results are given on two samples. For one sample, magnetoresistance of n^--type GaAs is due to magnetic localization. There is good agreement between experimental magnetoresistance measurements and the percolation theory of Shklovskii, Efros, and Ioselevich.[4,28] For the second sample, we observe a dip in C-V and G-V curves at flat-band voltage V_{FB} which we attribute to magnetic freezeout in n^--type GaAs. Although the mechanism responsible for the observation of magnetoresistance in n^--type GaAs differs for the two samples, the activation energies for magnetoresistance of the two samples are nearly identical in the range of B where the data overlap.

EXPERIMENT

Figure 1(a) shows schematically the energy-level diagram of the AlGaAs capacitors studied, biased into accumulation by a positive gate voltage V_G. Both samples were grown by molecular-beam epitaxy (MBE) on $\langle 100\rangle$ n^+-type GaAs wafers. Characteristics of the two samples are given in Table I. The substrate doping $N_S=N_D-N_A$ is derived from C-V curves in depletion.[34] The gate doping N_G, and the thickness w, of the undoped $Al_{0.4}Ga_{0.6}As$ layer are obtained by comparing C-V curves measured between 77 and 150 K with theoretical C-V curves calculated from classical semiconductor-insulator-semiconductor (SIS) theory.[34] A value of the dielectric constant of $Al_{0.4}Ga_{0.6}As$ of 11.8 at 300 K is assumed. The thickness derived from C-V curves when the substrate is accumulated is about 3 nm larger than the true insulator thickness.[35] The activation energy ϕ_G is obtained from the temperature dependence of I-V curves between 100 and 250 K where thermionic emission determines I-V curves.[34] The flat-band voltage V_{FB}, the value of V_G for which the electric field at the n^--type-GaAs/$Al_xGa_{1-x}As$ interface is zero, is obtained from C-V or G-V curves at low temperature. The run numbers are included since the same samples are used in other publications.[36] For both samples the n^--type GaAs substrate thickness was ~ 1.0 μm. N_A is not known for either sample. Si, the substrate dopant in both samples, is amphoteric in GaAs, but is primarily a donor under the

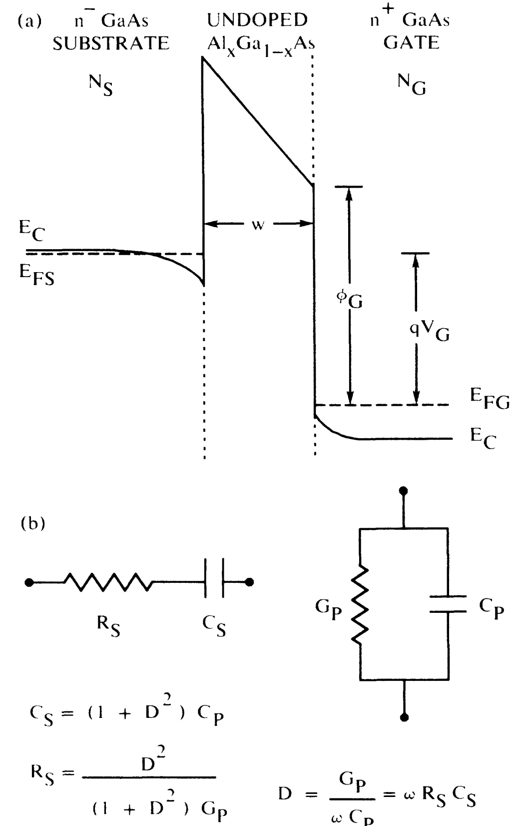

FIG. 1. (a) Schematic energy-band diagram for n^- type-GaAs-$Al_xGa_{1-x}As$-n^+-type-GaAs (AlGaAs) in accumulation. (b) Equivalent circuit representations for impedance of AlGaAs capacitor.

TABLE I. Properties of $Al_xGa_{1-x}As$ capacitors. N_S is the substrate doping, N_G is the gate doping, w is the $Al_xGa_{1-x}As$ thickness, V_{FB} is the flat-band voltage, and ϕ_G is the activation energy for thermionic emission.

Sample	Number	N_S (10^{15} cm^{-3})	N_G (10^{18} cm^{-3})	w (nm)	V_{FB} (V)	ϕ_G (eV)
A	1332*A*3	1.7	0.9	23.0	−0.030	0.320
B	432*C*6	7.0	1.8	21.0	−0.045	0.263

growth conditions. In addition, undoped GaAs grown by MBE tends to be p type with N_A in the range of $(3-7)\times10^{14}$ cm^{-3}. Values of compensation K of 0.1–0.5 are likely for both samples. After MBE growth Au-Ge-Ni Ohmic contacts were made to the n^+-type GaAs gate and to the n^+-type GaAs wafer and capacitors of 4.1×10^{-4} cm^2 area were formed by etching a mesa. Samples were mounted in 8-pin TO-5 transistor headers for measurement.

C-V and G-V curves were measured with a Hewlett-Packard HP4574A *LCR* meter.[31,34] Four-probe measurements were made in all cases. As shown in Fig. 1(b) the impedance of a SIS capacitor can be analyzed as either a parallel capacitance C_P and conductance G_P, or as a series capacitance C_S and resistance R_S. The *LCR* meter measures ac impedance of a capacitor as either a parallel or series circuit. The two representations of impedance are completely equivalent. Measurements have been made in the parallel configuration since these quantities are sensitive to structure due to Landau levels;[31] R_S and C_S are obtained from the formulas given in Fig. 1(b). In Fig. 1(b), D is the dissipation factor and ω is the measurement frequency in rad/s. R_S depends primarily on the resistivity of the n^--type GaAs layer. Values of R_S given throughout the paper can be converted to resistivities of n^--type GaAs, ρ_S, by multiplying by 4.13. Ideally the ac modulation voltage for C-V measurements should be less than kT/e. This is not feasible at 4.2 K or lower temperatures; instead, the modulation voltage was 0.004 V rms for all measurements. Impedance measurements are most accurate at high frequencies. However, above ~200 kHz the capacitance of leads going into the cryostat made accurate C-V measurements difficult, particularly at high magnetic fields. Most measurements have been made at 100 kHz, but some results are reported at frequencies as low as 1 kHz since higher values of R_S can be determined at lower frequencies. Two types of measurements were made. C-V and G-V curves were measured by changing V_G at fixed magnetic field B; C-V-B and G-V-B curves were made by measuring C and G at fixed V_G as the magnetic field was swept. In measuring C-V-B and G-V-B curves, between 12 and 16 gate voltages were sampled in cyclic fashion as B changed. Values of C and G at values of B between measured values are obtained by interpolation. Magnetic fields up to 15 T were obtained with a superconducting magnet. Temperatures were controlled between 1.4 and 4.2 K by immersing the sample in pumped liquid helium. Data acquisition was controlled by an IBM Series/1 computer.

RESULTS

Sample A

The substrate doping of sample A, 1.7×10^{15} cm^{-3}, is such that the theory of Shklovskii and Efos[4] can be expected to be valid. This is found to be the case. The results for sample A show that ac-impedance measurements of AlGaAs capacitors give quantitative data on magnetic localization in n^--type GaAs and establish the validity of the method.

When a magnetic field is applied perpendicular to an AlGaAs capacitor two-dimensional Landau levels form in the accumulation layer which cause structure in both C-V and G-V curves. Since the primary interest of the present paper is magnetoresistance of the n^--type GaAs substrate, all measurement have been made with B parallel to the sample unless otherwise stated. Under such conditions two-dimensional Landau levels do not form although three-dimensional Landau levels occur in both substrate and gate.[36,37] C-V curves for sample A at 100 kHz and at different magnetic fields applied parallel to the sample layers are shown in Fig. 2 and the corresponding G-V curves are shown in Fig. 3. The flat-band voltage for sample A is −0.030 V; at higher gate voltages an accumulation layer forms on the n^--type GaAs substrate. For the C-V curve at 0 T the maximum capacitance depends on the thickness of the AlGaAs dielectric and on band bending in both substrate and gate. The decrease in C at $V_G>0.15$ V depends primarily on band bending in the gate and thus on N_G.[34] As shown in Fig. 2, increasing B decreases the magnitude of capacitance, but there is no structure due to Landau levels in the accumulation layer. At 2 T the C-V curve is nearly the same as at 0 T; at 4 and 6 T the measured capacitance decreases due to the increased resistance of the substrate. Above 8 T the capacitance is nearly constant from negative gate voltages corresponding to depletion until there is a steep rise in C above ~0.3 V.

G-V curves corresponding to the C-V curves of Fig. 2 are shown in Fig. 3. The minimum G that can be measured at 100 kHz by the *LCR* meter is 10^{-8} S. For 0 T, $G\leq10^{-8}$ S for negative V_G. There is a peak in G at $V_G=-0.030$ V. This is followed by a plateau between 0.0 and 0.2 V and then a steep rise in G. At 2 T, G for $0.0<V_G<0.2$ V is an order of magnitude greater than at 0 T; at 4 T it is another decade larger than at 2 T. At higher values of B, the plateau value of G decreases with increasing B because of the increase of resistance of the GaAs substrate.

A significant problem in working with two-dimensional accumulation or inversion layers on semiconductors is identifying the threshold voltage for establishment of a two-dimensional layer.[38] For an accumulation layer on a SIS capacitor the problem is equivalent to identifying the flat-band voltage V_{FB}. One method of measuring V_{FB} is to measure the dependence of tunnel currents through the $Al_xGa_{1-x}As$ barrier on a magnetic field perpendicular to an AlGaAs capacitor. Minima occur in tunnel currents when the Fermi level of an accumulation layer passes through minima in the density of states that occur when Landau levels form.[31] For sample A the voltage for the conductance peak at 0 T in Fig. 3 is the same as V_{FB} derived from tunneling measurements when B is perpendicular to the sample.

A plateau in G and C for $0.0 \lesssim V_G \lesssim 0.15$ V is characteristic for sample A. In this voltage region the series circuit representation of the impedance of a SIS capacitor, as shown in Fig. 1(b), is very good. Physically, C_S is constant at a given value of V_G when the AlGaAs capacitor is in accumulation. C_S depends on the insulator capacitance C_I, and on the magnitude of band bending in substrate and gate; these depend only on V_G and are independent of B. R_S is the resistance of the n^--type GaAs substrate and is physically in series with C_S. The primary voltage drop for $V_G > V_{FB}$ is across the $Al_xGa_{1-x}As$ barrier; band bending in substrate and gate are approximately equal, and the voltage drop across the n^--type GaAs substrate is small.[35] The rise in G and in C above ~ 0.3 V is due to dc tunnel currents through the $Al_xGa_{1-x}As$ barrier which increase exponentially with V_G and become the dominant component of ac currents. (The I-V curve for sample A is plotted in Ref. 36.) In the rest of the paper we derive values of R_S from G_P and C_P measured at voltages corresponding to the region of constant C_P and G_P where the substrate is accumulated and dc tunnel currents do not dominate the ac conductance. Experimental values of R_S are plotted in subsequent figures; resistivity can be obtained by multiplying by 4.13. The general features of C-V curves are the same between 1 and 100 kHz. At a given value of B the measured capacitance in the plateau region is greater at lower frequencies since $1+D^2$ in the formulas of Fig. 1(b) is smaller. G-V curves at different frequencies also have a region of constant G in accumulation although the width of the plateau is smaller at lower frequencies since dc tunnel currents dominate ac conductance at lower voltages.

The detailed dependence of capacitance and conductance on magnetic field is shown by C-V-B and G-V-B curves in which C and G are measured at constant V_G as B changes. Figures 4(a) and 4(b) show such curves at 100 and 10 kHz and at a constant $V_G = 0.10$ V. The capacitance ratio, $C_P(B)/C_P(0)$, is plotted, in which $C_P(0)$ is the capacitance at V_G and low B where C_P is not reduced

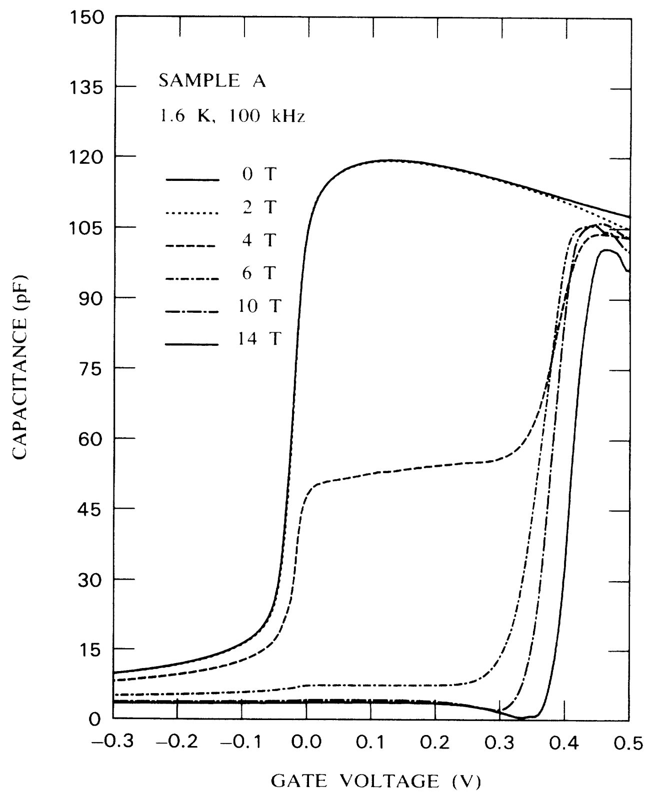

FIG. 2. Capacitance-voltage curves of sample A at 100 kHz at different magnetic fields. Magnetic field parallel to sample.

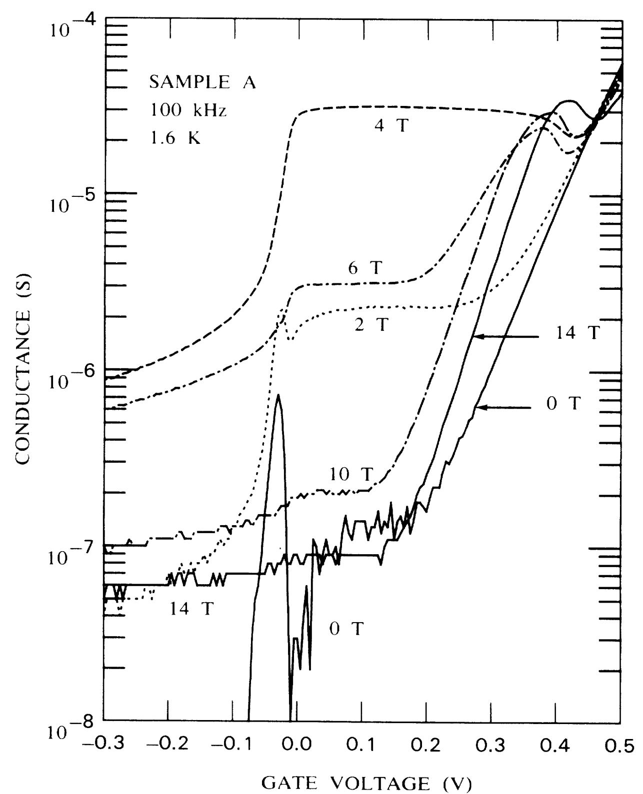

FIG. 3. Conductance-voltage curves of sample A at 100 kHz at different magnetic fields. Magnetic field parallel to sample.

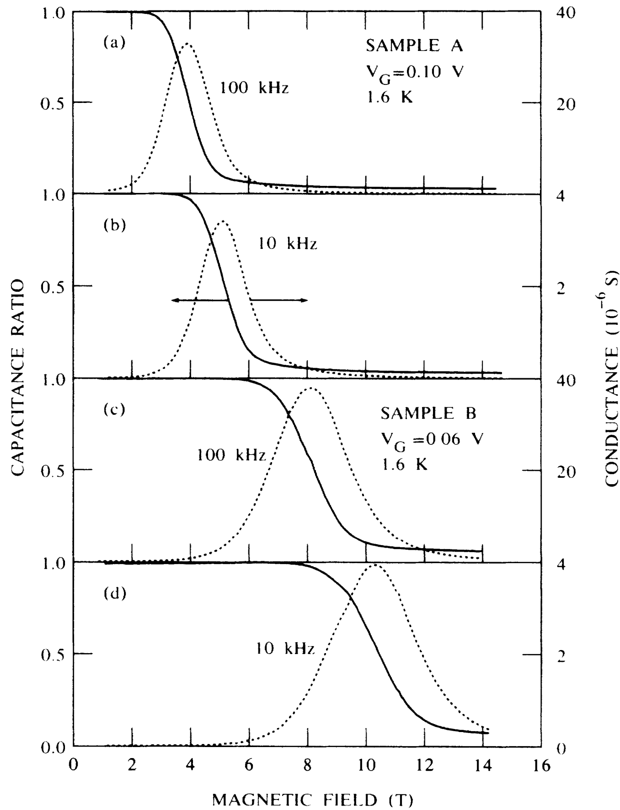

FIG. 4. (a),(b) Dependence of the ratio of capacitance at magnetic field B to the capacitance at 0 T on B, and of the conductance on B, for sample A at different frequencies. V_G is constant in each case. (c),(d) Similar curves for sample B.

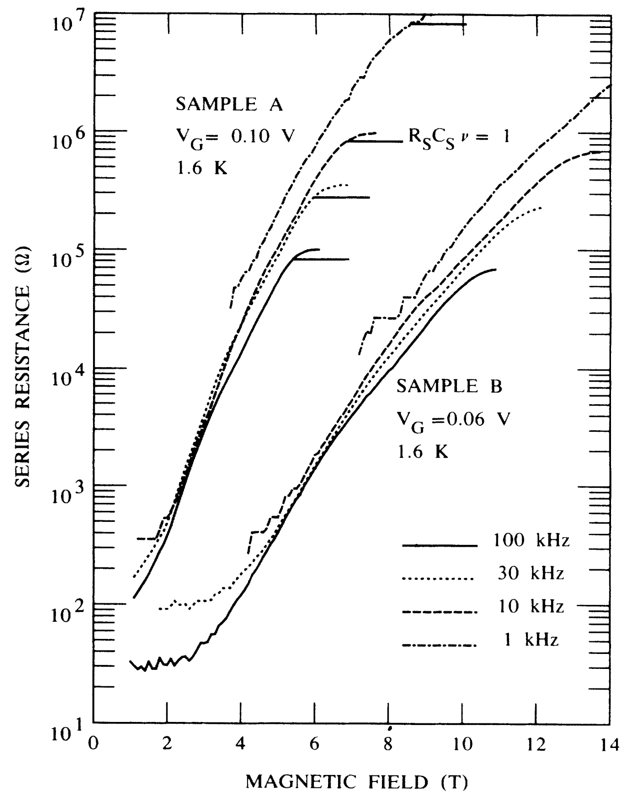

FIG. 5. Dependence of series resistance of n^--type GaAs on magnetic field for samples A and B for different frequencies and constant V_G. Horizontal lines show resistance at which $R_SC_S(0)\nu=1$.

by series resistance. Such a plot is convenient in comparing the dependence of C_P on B at different voltages or frequencies. Conductance is plotted on a linear scale; note that the scale is different for each frequency. The capacitance ratio decreases from 1.0 to $\sim$0.04 over a range of B of $\sim$3 T. G_P is characterized by a peak which occurs at higher B for lower frequency. For a given frequency and temperature plots of $C(B)/C_P(0)$ and G are independent of V_G for accumulation voltages that lie on the plateau region of Fig. 3.

Series resistance R_S, as a function of B, calculated for data such as in Fig. 4 by the equations of Fig. 1(b), is shown in Fig. 5. The exponential dependence of R_S on B which is characteristic of hopping conduction in lightly doped semiconductors is found. R_S at a given value of B is essentially independent of frequency. $C_S(0)$, the series capacitance at $B=0$ T, is equal to $C_P(0)$. The apparent leveling off of R_S at high B occurs when $R_SC_S(0)\nu>1$, as shown by the horizontal lines in Fig. 5. ν is the measurement frequency. The circuit cannot respond at higher resistances. Results at 1 kHz are only valid for $R_S>4\times10^4$ Ω. Low-frequency curves are inaccurate at low magnetic fields because of the minimum value of G that can be measured by the LCR meter.

Ioselevich has evaluated the expressions of Shklovskii and Efros for magnetoresistance due to hopping conduction.[28,29] He gives a curve for the critical exponent for percolation ξ^* as a function of a normalized magnetic field $B^*=B/B_C$, which is valid for arbitrary B. B_C is defined by Eq. 3. If $\rho(B)$ is the resistivity at magnetic field B and $\rho(0)$ is the resistivity in zero magnetic field,

$$\ln[\rho(B)/\rho(0)]=\xi_0(\xi^*-1)\ , \tag{1}$$

$$\xi_0=1.73/N_D^{1/3}a_H^*\ , \tag{2}$$

$$B_C=3.47N_D^{1/3}/\hbar ea_H^*\ . \tag{3}$$

Figures 6(a) and 6(b) show the data of Figs. 5(a) and 5(b) analyzed according to Eqs. (1)–(3). The solid curve is the curve given by Ioselevich and the dashed curves are from experimental data at two frequencies. Figure 6(a) also gives values of B that correspond to values of B^* for sample A. The agreement between theory and experiment is particularly good for the 10-kHz curve. At 100 kHz experiment deviates from theory above $\sim$4.2 T where $R_SC_S\nu\gtrsim1$. At 10 kHz the experimental curve does not fall below theory until $B^*>2.0$ The agreement between theory and experiment over a wide range of B^* is better than found previously for n^--type GaAs.[20,29] From this agreement we conclude that conduction at low

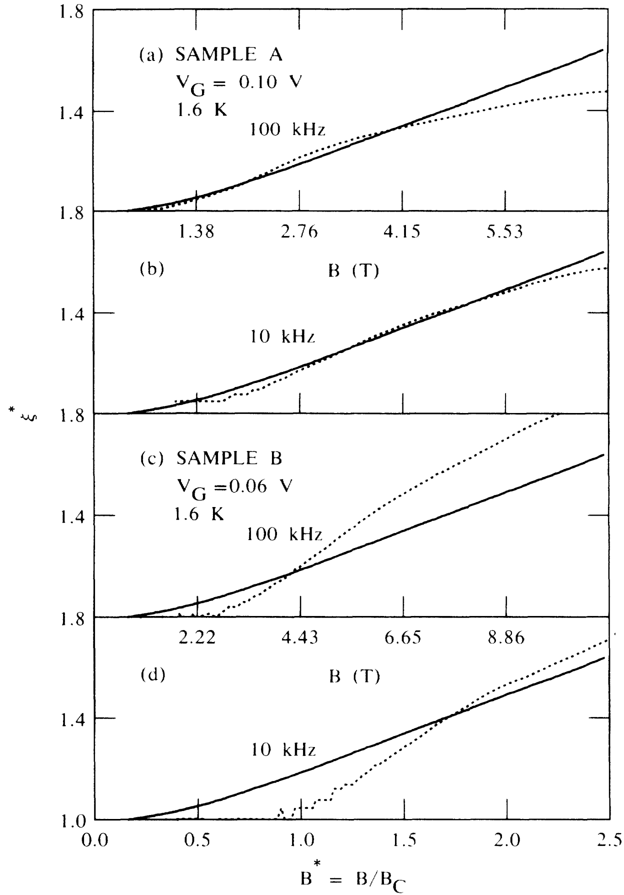

FIG. 6. (a),(b) Comparison of theoretical and experimental values of the critical exponent for percolation ξ^* on B^* for sample A at two frequencies. Solid line shows theoretical curve from Ref. 28; dashed line is experimental. Abscissa of (a) shows actual values of B. (c), and (d) show similar curves for sample B.

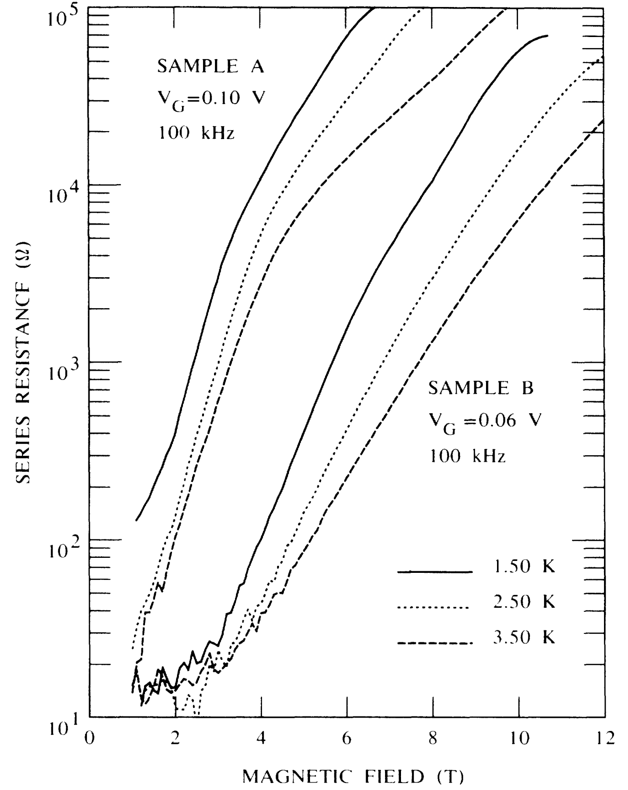

FIG. 7. Dependence of R_S of n^--type GaAs on magnetic field at different temperatures for sample A and for sample B.

temperature in the n^--type GaAs substrate of sample A is by hopping conduction through a donor band separated from the conduction band by $\sim E_D$. The Fermi level is in the lower impurity band for all values of magnetic field.[4]

ac conduction in sample A is thermally activated, both at 0 T and at higher magnetic fields. The temperature dependence of magnetoresistance of sample A at 100 kHz is shown in Fig. 7 in which R_S is plotted as a function of magnetic field for temperatures between 1.50 and 3.50 K. An exponential dependence of R_S on B is observed at all temperatures. The typical temperature dependence of the resistivity of lightly doped semiconductors in the hopping conduction regime is[39]

$$\rho(B)=\rho_3(B)\exp(\varepsilon_3/kT) . \quad (4)$$

The data for sample A are plotted according to Eq. (4) in Fig. 8. The lines in Fig. 8 are least-squares fits of the data for $0.3 \le 1/T \le 0.5\ \mathrm{K}^{-1}$. The data in Fig. 8 are in accord with hopping conduction, for which ε_3 is the activation energy and ρ_3 depends on B. The value of ε_3 in meV is shown in Fig. 9(b) and the preexponential factor $R_3(B)$ is shown in Fig. 9(a). $R_3(B)$ is obtained from Fig. 8 by extrapolating to $1/T=0\ \mathrm{K}^{-1}$. Figure 9(b) also shows ε_3 at 0 T. Data for Fig. 9(b) have been calculated at 0.1-T intervals; the vertical lines show the standard deviation of the least-squares data fitted at 0.5-T intervals. At very low temperatures and low doping, variable-range hopping is observed in GaAs; conduction varies as $\exp(-T/T_0)^s$, where s is $\frac{1}{2}$ or $\frac{1}{4}$.[14,15] R_S at the lowest temperatures in Fig. 8 is nearly independent of temperature. This is the temperature range for variable-range hopping, but the data are not accurate enough, nor do they go to low enough temperatures, to tell if variable-range hopping occurs or to obtain the exponent s for variable-range hopping. Figure 9 shows ε_3 and $R_3(B)$ for $V_G=0.10$ V; similar results are obtained for $0.010 \le V_G \le 0.13$ V, including an apparent peak in ε_3 at 3.2 T and a minimum at 4.5 T. The values of ε_3 are similar to those reported previously for hopping conduction in GaAs.[8,10,11,13] Figure 6 compares experiment and theory at 1.6 K. The same agreement with theory is observed up to 3.5 K; at higher temperature $R_S(0)$ appears to be constant due to lack of sensitivity of the LCR meter. Using values of $R_S(B)/R_S(0)$ to calculate ξ^* is then of uncertain accuracy.

For low magnetic fields, Shklovskii and Efros[23] show that

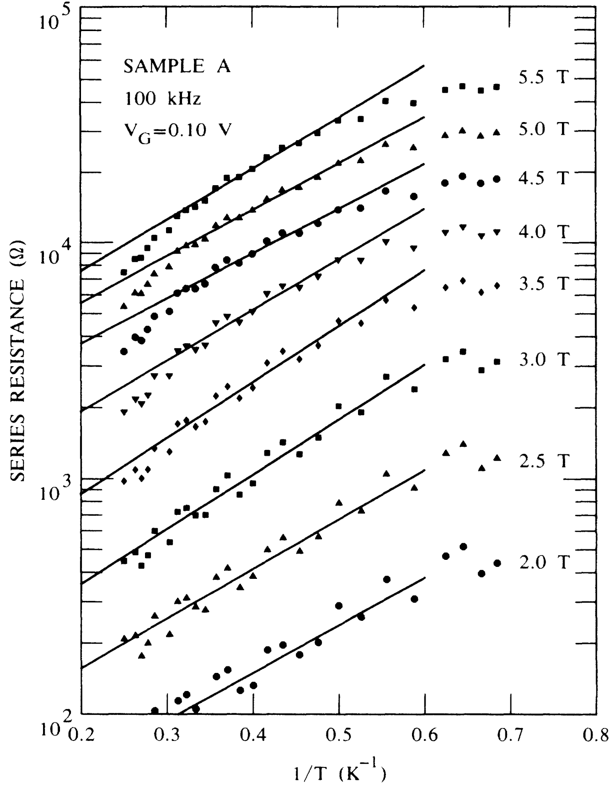

FIG. 8 Dependence of R_S at 100 kHz of n^--type GaAs on $1/T$ at different values of B for sample A. Solid lines are least-squares fit of data for $0.3 \leq 1/T \leq 0.5$ K^{-1}.

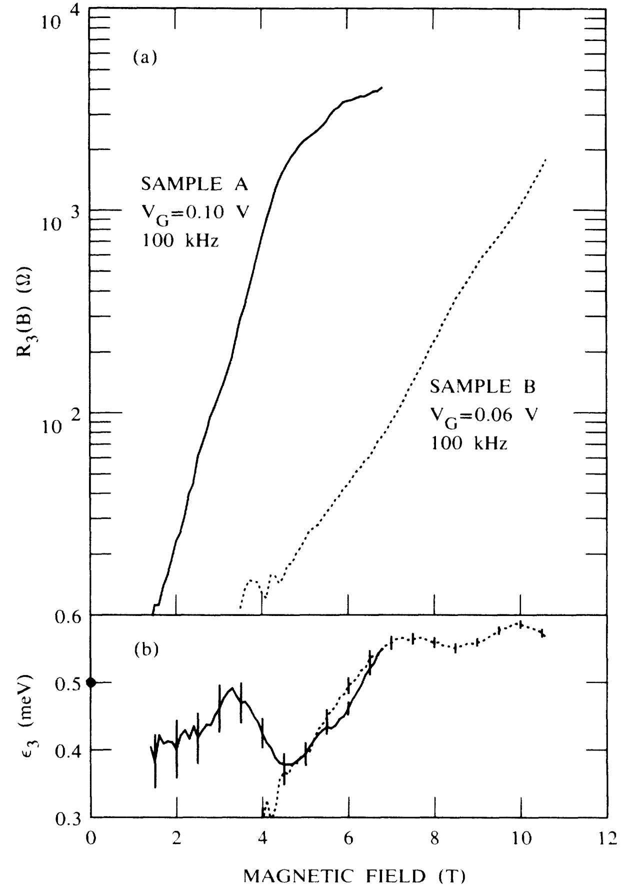

FIG. 9. (a) Dependence of $R_3(B)$ at constant V_G and 100 kHz on B for samples A and B. (b) Dependence of ε_3 at constant V_G and 100 kHz on B for samples A and B. Vertical lines are standard deviation of least-squares fit of data.

$$\rho_3(B)/\rho_3(0)=\exp\left[t\frac{ae^2}{N_S\hbar^2}B^2\right]. \quad (5)$$

From percolation theory they calculate that $t=0.036$. The experimental ratio $\ln[R_3(B)/R_3(0)]$ is proportional to B^2 for $B^2<6$, where $R_3(B)$ is given in Fig. 9(a). The value of t is 0.036–0.039, which is in excellent agreement with the value of Shklovskii and Efros.

A characteristic feature of the percolation model of magnetic localization in three dimensions is that the longitudinal and transverse magnetoresistance are nearly equal. The results on sample A correspond to transverse magnetoresistance since the ac current flows from the n^+-type GaAs wafer through the n^--type GaAs substrate into the accumulation layer at the GaAs/$Al_xGa_{1-x}As$ interface and **B** is perpendicular to this current. Longitudinal magnetoresistance is observed when **B** is perpendicular to the sample and parallel to current flow. Figure 10 shows that the two magnetoresistences are essentually equal at 100 kHz and 1.7 K for $B \leq 5$ T. Structure for **B** perpendicular to the sample is due to the effect of Landau levels in the accumulation layer.

Sample B

The principal difference between sample A and sample B is that the substrate doping of sample B is about 4 times higher than that of sample A. The fact that the $Al_xGa_{1-x}As$ thickness is smaller, the gate doping is higher, and the barrier height for thermionic emission is lower is of secondary importance. Instead of exhibiting magnetic localization as sample A does, sample B has an exponential magnetoresistance due to magnetic freezeout of carriers.

C-V and G-V curves for sample B at 100 kHz and different magnetic fields are shown in Figs. 11 and 12. As for sample A, capacitance decreases at high magnetic fields. However, values of B greater than 6 T are required for capacitance in accumulation to decrease from its value at 0 T. There is a plateau region for both C and G between 0.0 and 0.1 V, as there is for sample A. The rise in ac conductance due to dc tunnel current occurs at lower voltage than for sample A because of the thinner $Al_xGa_{1-x}As$ dielectric layer. The peak in conductance at V_{FB} which occurs at 0 T for sample A is not found for sample B, but peaks at -0.055 V are found for G-V curves at 2 and 4 T.

The distinctive feature of the C-V curves of Fig. 11 is the dip in capacitance at magnetic fields greater than ~ 6 T that is apparent at -0.050 V. This is a Gray-Brown

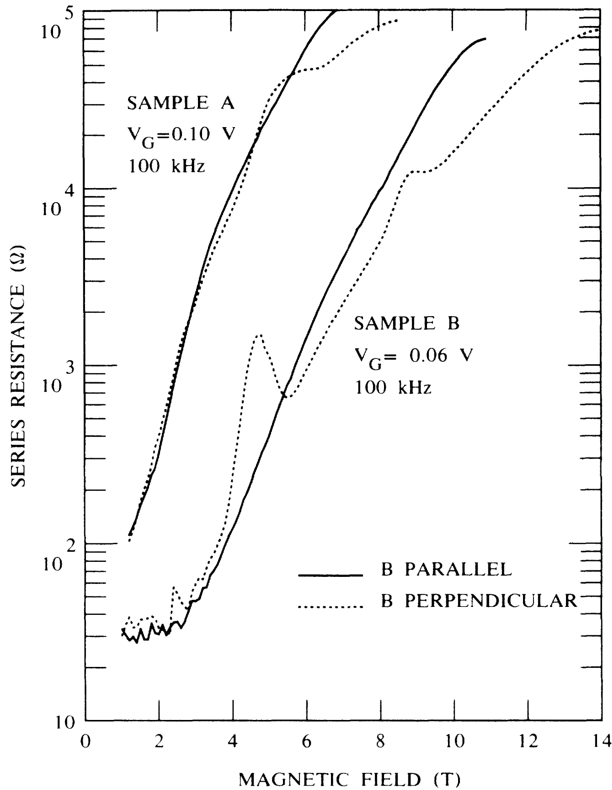

FIG. 10. Dependence of R_S of n^--type GaAs for samples A and B on B for B parallel and perpendicular to plane of sample. $T=1.7$ K.

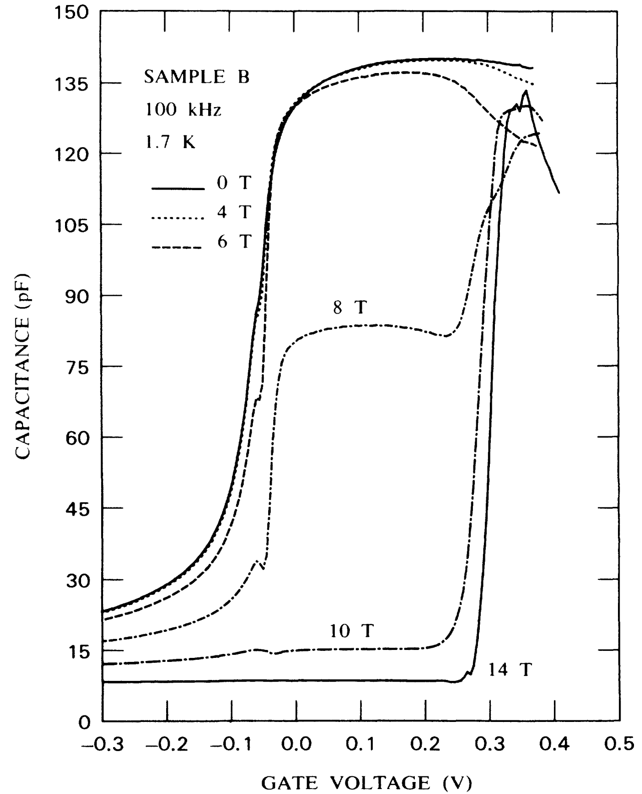

FIG. 11. Capacitance-voltage curves of sample B at 100 kHz at different magnetic fields. Magnetic field parallel to sample.

(GB) dip due to magnetic freezeout of carriers in the n^--type GaAs substrate.[40–43] The GB dip has been observed for thermal freezeout of carriers in silicon metal-oxide-semiconductor (MOS) capacitors. It has not previously been observed for magnetic freezeout of carriers in semiconductors. The GB dip occurs at a voltage equal to or very close to the flat-band voltage; if it can be observed in an MOS or SIS capacitor, it is one of the most accurate methods of determining V_{FB}. The minimum of the dip coincides with V_{FB}, obtained by plotting the magnetic fields for Landau-level minima, observed for dc I-V curves with B perpendicular to the sample, against V_G.[31] The voltage for the GB dip is independent of frequency; both C-V and G-V curves have dips at V_{FB} at frequencies between 1 and 100 kHz. At a given value of V_G series resistance decreases measured values of parallel capacitance at higher frequencies but, as for sample A, there is a plateau region at all frequencies where both C and G are nearly constant.

A GB dip occurs in C-V curves when the carrier concentration of a sample is such that the bulk Fermi level coincides with a donor (or acceptor) level in the semiconductor. In an ideal semiconductor the Fermi level of an n-type semiconductor at low temperatures lies between the conduction band and the donor level. (This disregards the possibility that the Fermi level in a compensated semiconductor is pinned in an impurity band, as for sample A.) As the temperature is lowered freezeout of carriers occurs, reducing the carrier concentration below the impurity concentration; the Fermi level moves towards the impurity level and eventually coincides with it. Filling and emptying the impurity level at the semiconductor-insulator interface at the ac measuring frequency produces a capacitance that is in series with the insulator capacitance and the depletion-layer capacitance; the result is a dip in the total capacitance.

Although a dip due to thermal freezeout in the n^--type GaAs substrate is not seen in sample B, there is a reproducible inflection at V_{FB} in the experimental C-V curve at 0 T that may be due to deionization of an impurity level; the inflection becomes a dip at magnetic fields greater than 6 T at which magnetic freezeout can occur in GaAs.[30] Theoretically, the position of the GB dip depends only on N_D, not on N_A.[41] In Fig. 13, C-V curves at 1 kHz and different B are shown; the series resistance at 1 kHz is low enough that the measured value of maximum capacitance is nearly as large at 10 T as at 0 T. The GB dip shifts to lower capacitances and the C-V curves become progressively steeper as B increases while V_{FB} remains constant. This behavior is qualitatively what the classical SIS model predicts should occur if N_D decreases due to freezeout of carriers.

C-V-B and G-V-B curves for sample B are shown in Figs. 4(c) and 4(d) for $V_G=0.060$ V and two different fre-

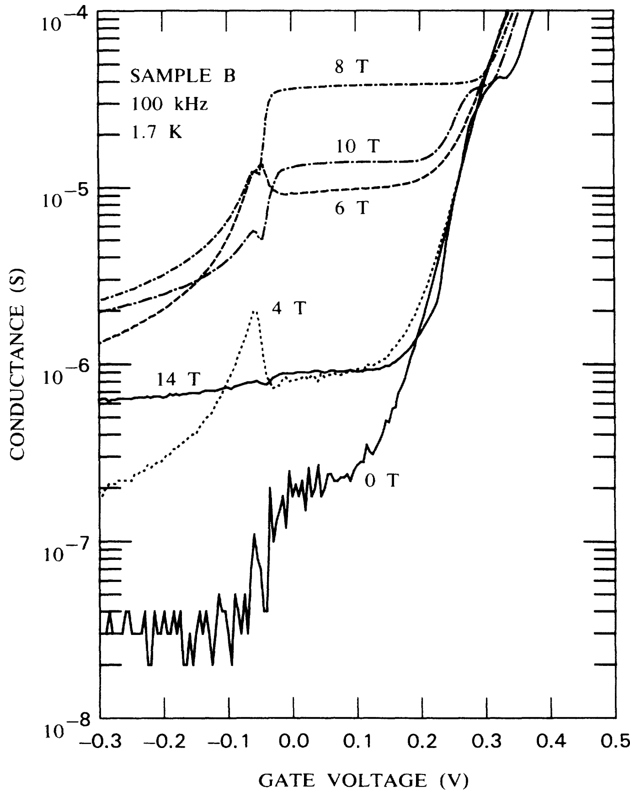

FIG. 12. Conductance-voltage curves of sample B at 100 kHz at different magnetic fields. Magnetic field parallel to sample.

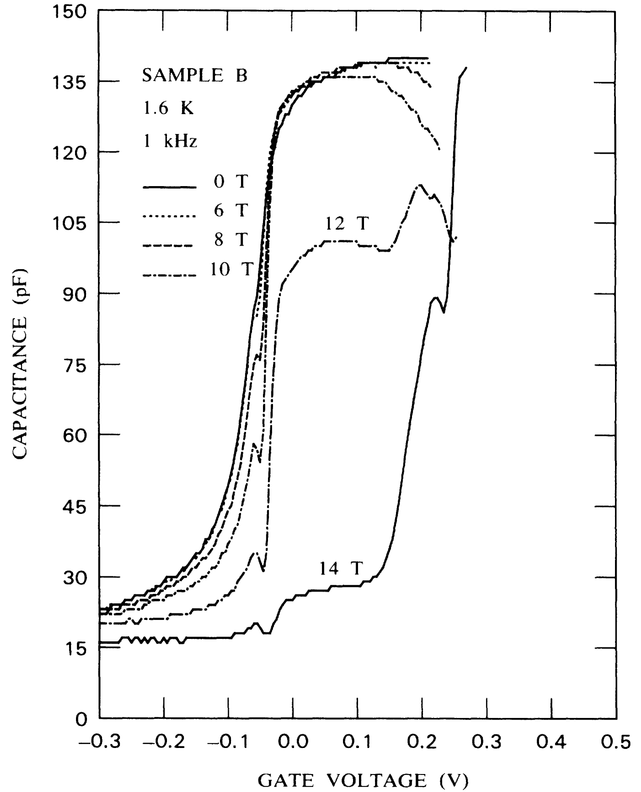

FIG. 13. Capacitance-voltage curves for sample B at constant frequency of 1 kHz and at different magnetic fields parallel to sample.

quencies. The curves are similar to those for sample A, but are shifted to higher magnetic fields in accordance with the higher substrate doping and lower series resistance. At any frequency C-V-B and G-V-B curves are nearly identical for $0.0 \leq V_G \leq 0.10$ V. Series resistance at $V_G = 0.060$ V and different frequencies are shown in Fig. 5. The cutoff value of R_S at high magnetic field corresponds to $R_S C_S \nu \gtrsim 1$. As for sample A, the maximum values of R_S that can be measured are determined by the condition that $R_S C_S \nu = 1$.

Although the resistance of sample B is exponential in B, it does not fit the analysis of Eqs. (1)–(3). Figures 6(c) and 6(d) show the data of Fig. 5 plotted according to Eqs. (1)–(3). The data are cut off at low values of B^* since measured values of R_S are not accurate at low B. Contrary to the results for sample A there is a poor fit of data for sample B to the percolation theory of Shklovskii, Efros, and Ioselevich. Thus, from the occurrence of a GB dip in C-V curves of sample B in magnetic fields greater than ~ 6 T, we conclude that magnetic freezeout occurs; freezeout lowers the Fermi level until it is in a donor level which can fill and empty at the measurement frequency when $V_G = V_{FB}$.

As is the case for sample A, the magnetoresistance of sample B is thermally activated. Figure 7 shows series resistance of sample B at 100 kHz as a function of B for different temperatures. There is a region of B below 3 T where R_S appears to be constant. This is the minimum value of R_S that can be accurately measured; it reflects the minimum conductance that can be measured by the LCR meter. Contrary to results on sample A, there is no evidence for any dependence of R_S at 0 T on temperature for sample B. As for sample A, activation energies for resistance are obtained by plotting the logarithm of R_S versus $1/T$ at constant values of B. The general pattern of temperature dependence of resistance is similar to that of sample A, although higher values of B are required to produce comparable values of R_S. Equation (4) is obeyed between 2 and 3 K. At lower temperatures R_S is nearly constant with temperature though with scatter of the data. Figure 9(a) shows $R_3(B)$ and Fig. 9(b) shows ε_3 for sample B. The standard deviation of the least-squares fit of the data is shown by vertical lines in Fig. 9(b). Although there are significant differences in the magnetoresistive behavior of samples A and B, there is a remarkably close agreement in ε_3 in the region between 4.5 and 6.5 T where the data overlap. There is a maximum in ε_3 at ~ 7.2 T and at ~ 10.0 T for sample B. The values of R_3 and ε_3 for sample B are given up to 11 T. Even at the lowest temperatures used to derive R_S and ε_3, R_S is less than the value for which $R_S(B)C_S(0)\nu = 1$ but it is getting close. This may mean that the actual value of B for a maximum for ε_3 is somewhat higher than 10.0 T since the effect of series resistance that is too large is to

give lower apparent values for ε_3. The value of ε_3 of 0.5–0.6 meV for both samples A and B is in good agreement with earlier data,[8,10,11] which also found ε_3 nearly independent of N_S.

Contrary to the results for sample A, the series resistance with the magnetic field perpendicular to sample B differs appreciably from that with the magnetic field parallel to the sample, as shown in Fig. 10. However, a similar GB dip occurs in C-V curves for B perpendicular, showing that the dependence of Fermi level on magnetic field is similar for the two orientations. This provides further evidence that the origin of magnetoresistance is different for the two samples although in both cases magnetoresistance is exponentially dependent on B.

DISCUSSION

Magnetoresistance of both samples A and B has been measured in a magnetic field parallel to the sample to avoid effects due to Landau levels in the two-dimensional electron gas in an accumulation layer. In such a magnetic field the energy of the conduction-band minimum E_C increases by $\hbar\omega_c/2$ and a series of bulk Landau levels develops whose energies are given by

$$E = E_C + (N + \tfrac{1}{2})\hbar\omega_c, \quad N = 0,1,2,\ldots . \tag{6}$$

Equation (6) neglects spin terms since the bulk g value for GaAs is small. There is also a small increase in the donor-level separation from the conduction band which is proportional to B^2.[30,44,45] Figure 14(a) shows a schematic band diagram for a semiconductor in a magnetic field using parameters that are appropriate for n^--type GaAs; it ignores the increase of donor binding for high values of B.

Previous work on magnetoresistance of lightly doped GaAs has shown that hopping conduction occurs in compensated n^--type GaAs.[23] For bulk GaAs, the activation energy ε_3 is 0.4–0.5 meV and is nearly constant for $N_S = N_D - N_A$ between 1×10^{15} and $\sim 8\times10^{15}/\text{cm}^3$.[8] At higher values of N_S, ε_3 decreases to zero at approximately the value of N_S for the metal-insulator transition in n^--type GaAs, $2\times10^{16}/\text{cm}^3$. The constancy of ε_3 with increasing N_S is not explained by percolation theory, which predicts[39] that (mks units)

$$\varepsilon_3 = 0.99e^2\frac{N_D^{1/3}}{4\pi\epsilon\epsilon_0}(1-0.3K^{1/4}), \quad K \ll 0.2$$

or

$$\varepsilon_3 = C_1 e^2\frac{N_D^{1/3}}{4\pi\epsilon\epsilon_0}(1-K)^{-1/3}, \quad K \gg 0.5 ,$$

where $C_1 \sim 1$.

The values of ε_3 from the present work, 0.4–0.5 meV, are essentially the same for both samples A and B although N_D differs by about a factor of 4; they agree well with earlier measurements.[8,11] As shown in Figs. 6(a) and 6(b), conduction in sample A is by hopping in an impurity band. Magnetoresistance is due to magnetic localization in a compensated semiconductor. In Fig. 9(b) one of the most striking observations about ε_3 for sample A is that there is a peak in its value at 3.2 T. As shown in Fig. 14(a), this is the value of B for which $\hbar\omega_c = E_D$ for GaAs.

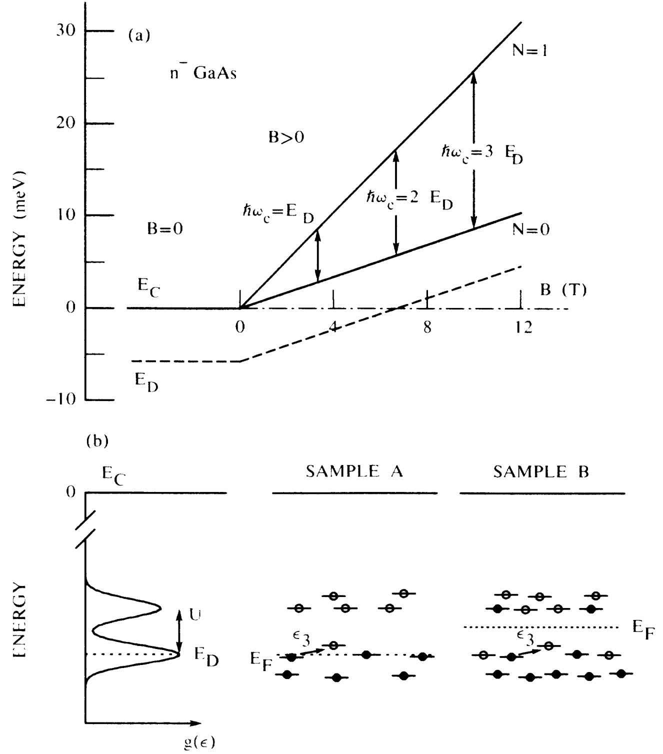

FIG. 14. (a) Schematic energy diagram of dependence of energy bands and donor level on magnetic field for n^--type GaAs. (b) Expanded schematic energy-band diagram showing impurity bands and relative positions of Fermi levels for samples A and B.

The appearance of a GB dip in C-V curves at magnetic fields above 6 T in sample B shows that magnetic freezeout occurs and, by analogy with observations of thermal freezeout,[40–43] provides evidence for a band structure for the sample. Although the mechanisms of magnetoresistance differ for samples A and B, the values of ε_3 are remarkably close for magnetic fields between 4.5 and 6 T where measurements on the two samples overlap, as shown in Fig. 9(b). There are peaks in ε_3 for sample B at 7.2 and 10.0 T. The former is a field at which $\hbar\omega_c$ is slightly greater than $2E_D$; the latter is somewhat greater than the value of B for which $\hbar\omega_c = 3E_D$, as shown in Fig. 14(a). There is no obvious reason for any resonant dependence of ε_3 on magnetic field. It may be related in some way to magnetoimpurity resonances (MIR's) in III-V compounds which have been reviewed by Eaves and Portal.[46] MIR phenomena, however, depend on having current flow in the sample; the magnitude of current for AlGaAs capcitors in accumulation is small.

Figure 14(b) is an attempt to show schematically common features of samples A and B that may cause values of ε_3 to be the same. The left-hand side of Fig. 14(b) shows a schematic distribution of the density of states, with two bands, placed at about the donor energy. $g(\varepsilon)$ is the density of states at energy ε. There are several

models that predict that there should be lower- and higher-energy states (or bands) for an impurity band. These include a Coulomb gap at the Fermi level of an impurity band,[47–49] D^+ and D^- bands which Fritzsche has invoked to explain impurity conduction in Ge,[50] and the Mott-Hubbard model of localization in which there is a lower and an upper Hubbard band separated by an energy U.[51] For sample A the Fermi level is in the lower band for all values of B. Acceptors that provide compensation are not shown since they would be deep in the gap on the scale of the figure. The activation energy for hopping conduction is customarily considered to be ε_3, the energy for an electron to jump from a filled state to the nearest empty state in the impurity band.

The carrier density for sample B is about 4 times larger than for sample A. In the schematic energy diagram for sample B the Fermi level is initially between the lower and the upper impurity band. In the Mott-Hubbard model, the energy U decreases as N_D increases until it becomes zero at the metal-insulator transition.[51] Within the accuracy of the measurements the resistance of sample B at 0 T is independent of temperature down to 1.45 K. As B increases, magnetic freezeout reduces the number of electrons in the upper band and the Fermi level moves into the lower band at the donor energy. At higher values of B the resistance of the sample increases further due to magnetic localization; the value of ε_3 is constant and the same as for sample A because ε_3 in both cases is the energy for hopping conduction in the lower band. The model of Fig. 14(b) is similar to that proposed by Sites and Nedoluha.[13] The origin of two bands is uncertain. Both the Mott-Hubbard bands and the D^+-D^- bands involve an impurity band interacting with the conduction band. The value of ε_3 is too small for carriers to be excited into the conduction band, particularly in sample A where $N_S = 1.7\times10^{15}$ cm^{-3}. Instead, the impurity level at the donor energy splits into two bands, and ε_3 is the activation energy for hopping conduction in the lower impurity band.

CONCLUSIONS

The conventional method of studying the temperature dependence of conduction and magnetoresistance in lightly doped semiconductors has been to combine dc-conduction and Hall-effect measurements to determine carrier concentrations and mobilities. The present work shows that C-V and G-V measurements of SIS capacitors provide an alternate method of studying magnetoresistance. The results for sample A agree well with the impurity conduction model of Shklovskii, Efros, and Ioselevich. They validate the method for samples with low doping in which magnetic localization occurs. The results for sample B show that magnetic freezeout occurs in higher doped samples. The change of Fermi level in the sample, its decrease due to magnetic freezeout, and its eventual coincidence with the lower impurity band are shown by the appearance of a GB dip at V_{FB} in C-V and G-V curves for $B > 6$ T. These results show that the Fermi level lies between an upper and lower impurity band at carrier concentrations that are less than half of that for the metal-insulator transition in n^--type GaAs. The disadvantage of ac-impedance methods is their lack of accuracy when sample resistance is low, i.e., at low magnetic fields and high temperatures. It is not clear if the accuracy is good enough to study magnetoresistance in the variable-hopping regime.

ACKNOWLEDGMENTS

The author would like to thank H. Morkoç for providing sample A, S. L. Wright for growing sample B, and D. C. LaTulipe for processing it into capacitors, F. F. Fang for making the superconducting magnet available, and F. Stern and M. Heiblum for discussions and review of the manuscript.

[1]M. Pepper, J. Non-Cryst. Solids **32**, 161 (1979).

[2]M. Pepper, in *Localisation and Interaction, Proceedings of the Thirty First Scottish Universities Summer School in Physics, 1986,* edited by D. M. Finlayson, (SUSSP, Edinburgh, 1986), p. 291.

[3]J. L. Robert, A. Raymond, R. Aulombard, C. Bousquet, and A. Joullie, in *The Application of High Magnetic Fields in Semiconductor Physics, Wurzburg, 1976,* edited by G. Landwehr, (Physikalisches Institut der Universität Würzburg, Würzburg, 1976), p. 533.

[4]B. I. Shklovskii and A. L. Efros, *Electronic Properties of Doped Semiconductors* (Springer-Verlag, Berlin, 1984).

[5]L. Halbo and R. J. Sladek, Phys. Rev. **173**, 794 (1968).

[6]S. Asai, T. Toyabe and M. Hirao, in *Proceedings of the Tenth International Conference on Semiconductors, Cambridge, 1970,* edited by S. P. Keller, J. C. Hensel, and F. Stern (U. S. AEC, Washington, D. C., 1970), p. 578.

[7]V. F. Dvoryankin, O. V. Emel'yanenko, D. N. Nasledov, D. D. Nedeoglo, and A. A. Telegin, Fiz. Tekh. Poluprovdn. **5**, 1882 (1971) [Sov. Phys.—Semicond. **5**, 1636 (1972)].

[8]O. V. Emel'yanenko, T. S. Lagunova, D. N. Nasledov, D. D. Nedeoglo, and I. N. Timchenko, Fiz. Tekh. Poluprovdn. **7**, 1919 (1973) [Sov. Phys.—Semicond. **7**, 1280 (1974)].

[9]H. Kahlert, *The Application of High Magnetic Fields in Semiconductor Physics, Wurzburg, 1974,* edited by G. Landwehr (Physikalisches Institut der Universität Würzburg, Würzburg, 1974), p. 470.

[10]H. Kahlert, G. Landwehr, A. Schlachetzki, and H. Salow, Z. Phys. B **24**, 361 (1976).

[11]D. Lemoine, C. Pelletier, S. Rolland, and R. Granger, Phys. Lett. **56A**, 493 (1976).

[12]G. A. Matveev, Fiz. Tekh. Poluprovdn. **15**, 2333 (1981) [Sov. Phys.—Semicond. **15**, 1355 (1981)].

[13]J. R. Sites and A. K. Nedoluha, Phys. Rev. B **24**, 4309 (1981).

[14]M. Benzaquen and D. Walsh, Phys. Rev. B **30**, 7287 (1984).

[15]R. Rentzsch, K. J. Friedland, A. N. Ionov, M. N. Matveev, I. S. Shlimak, C. Gladun, and H. Vinzelberg, Phys. Status Solidi B **137**, 691 (1986).

[16]D. Redfield, Adv. Phys. **24**, 463 (1975).

[17]T. G. Castner, Philos. Mag. B **42**, 873 (1980).

[18]T. G. Castner, W. N. Shafarman, and D. Koon, Philos. Mag. B **56**, 805 (1986).
[19]L. Eaves, P. S. S. Guimaraes, P. C. Main, I. P. Roche, J. A. Chroboczek, H. Mitter, J. C. Portal, and G. Hill, J. Phys. C **17**, L345 (1984).
[20]J. A. Chroboczek, L. Eaves, P. S. S. Guimaraes, P. C. Main, I. P. Roche, H. Mitter, J. C. Portal, P. N. Butcher, M. Ketkar, and S. Summerfield, in *Proceedings of the Seventeenth International Conference on Semiconductors,* edited by J. D. Chadi and W. A. Harrison (Springer-Verlag, Berlin, 1985), p. 697.
[21]R. Buczko, J. A. Chroboczek, and G. Wunner, Philos. Mag. Lett. **56**, 251 (1987).
[22]P. P. Edwards and M. J. Sienko, Phys. Rev. B **17**, 2575 (1978).
[23]See Ref. 4, Chap. 7.
[24]B. I. Shklovskii, Zh. Eksp. Teor. Fiz. **61**, 2033 (1971) [Sov. Phys.—JETP **34**, 1084 (1972)].
[25]B. I. Shklovskii, Fiz. Tekh. Poluprovdn. **6**, 1197 (1972) [Sov. Phys.—Semicond. **6**, 1053 (1973)].
[26]B. I. Shklovskii, Fiz. Tekh. Poluprovdn. **17**, 2055 (1983) [Sov. Phys.—Semicond. **17**, 1311 (1983)].
[27]M. Pollak, in *The Metal Non-Metal Transition in Disordered Systems, Proceedings of the Nineteenth Scottish Universities Summer School in Physics, 1978,* edited by L. R. Friedman and D. P. Tunstall (SUSSP, Edinburgh, 1978), p. 95.
[28]A. S. Ioselevich, Fiz. Tekh. Poluprovdn. **15**, 2373 (1981) [Sov. Phys.—Semicond. **15**, 1378 (1981)].
[29]J. A. Chroboczek, in *Applications of High Magnetic Fields in Semiconductor Physics,* Vol. 177 of Lecture Notes in Physics, edited by G. Landwehr (Springer-Verlag, Berlin, 1983), p. 396.
[30]Y. Yafet, R. W. Keyes, and E. N. Adams, J. Phys. Chem. Solids **1**, 137 (1956).
[31]T. W. Hickmott, Phys. Rev. B **32**, 6531 (1985).
[32]T. W. Hickmott, P. M. Solomon, F. F. Fang, F. Stern, R. Fischer, and H. Morkoç, Phys. Rev. Lett. **52**, 2053 (1984).
[33]L. Eaves, D. K. Maude, F. W. Sheard, and G. A. Toombs, in *High Magnetic Fields in Semiconductor Physics,* Vol. 71 of *Solid-State Sciences* edited by G. Landwehr (Springer-Verlag, Berlin, 1987), p. 319.
[34]T. W. Hickmott, P. M. Solomon, R. Fischer, and H. Morkoç, J. Appl. Phys. **57**, 2844 (1985).
[35]T. W. Hickmott, P. M. Solomon, R. Fischer, and H. Morkoç, Appl. Phys. Lett. **44**, 90 (1984).
[36]T. W. Hickmott, Solid State Commun. **63**, 371 (1987).
[37]B. R. Snell, K. S. Chan, F. W. Sheard, L. Eaves, G. A. Toombs, D. K. Maude, J. C. Portal, S. J. Bass, P. Claxton, G. Hill, and M. A. Pate, Phys. Rev. Lett. **59**, 2806 (1987).
[38]A. B. Fowler and A. M. Hartstein, Surf. Sci. **98**, 169 (1980).
[39]See Ref. 4, Chap. 8.
[40]P. V. Gray and D. M. Brown, Appl. Phys. Lett. **13**, 247 (1968).
[41]C. T. Sah, Solid State Electronics Laboratory Report No. 1, Electrical Engineering Laboratory, University of Illinois, 1964, p. 62 (unpublished).
[42]S. Aymeloglu and J. N. Zemel, IEEE Trans. Electron. Devices **ED-23**, 466 (1976).
[43]J. Snel, Solid-State Electron. **24**, 135 (1981).
[44]W. Rühle and E. Göbel, Phys. Status Solidi B **78**, 311 (1976).
[45]F. Willmann, W. Dreybrodt, M. Bettini, E. Bauser, and D. Bimberg, Phys. Status Solidi B **60**, 751 (1973).
[46]L. Eaves and J. C. Portal, J. Phys. C **12**, 2809 (1979).
[47]B. I. Shklovskii and A. L. Efros, Fiz. Tekh. Poluprovdn. **14**, 825 (1980) [Sov. Phys.—Semicond. **14**, 487 (1980)].
[48]B. I. Shklovskii and A. L. Efros, in *Electron-Electron Interactions in Disordered Systems,* edited by A. L. Efros and M. Pollak (North-Holland, New York, 1985), p. 409
[49]M. Pollak and M. Ortuno, Ref. 48, p. 297.
[50]H. Fritzsche, in *The Metal Non-Metal Transition in Disordered Systems, Proceedings of the Nineteenth Scottish Universities Summer School in Physics, 1978,* edited by L. R. Friedman and D. P. Tunstall (SUSSP, Edinburgh, 1978), p. 193.
[51]N. F. Mott and E. A. Davis, *Electronic Processes in Non-Crystalline Materials,* 2nd ed. (Oxford University Press, Oxford, 1979), p. 104.